

## Confinement Stabilises Single Crystal Vaterite Rods

Anna S. Schenk, Eduardo J. Albarracin, Yi-Yeoun Kim, Johannes Ihli, and Fiona C. Meldrum

### Table of Contents

- (1) *Experimental Methods*
- (2) *Supplementary Figures*
- (3) *Supplementary Tables*
- (4) *Characterisation of Track-Etch Membranes*
- (5) *Early Stage Analysis of Precipitation Mechanism*

### (1) Experimental Methods

Calcium carbonate nano-rods were precipitated in polycarbonate track-etched (TE) membranes with nominal pore sizes of 200 nm purchased from two different suppliers. The reactions were performed at ambient conditions according to a protocol established by Kim et al,<sup>1</sup> and a minimum of three repeats were carried out. Morphologies and surface textures of the intra-membrane particles isolated from the porous templates were characterised by electron microscopy. Selected area electron diffraction was performed on individual rods for polymorph identification and in order to study the crystallinity. For further confirmation of the polymorph, Raman microscopy and infra-red spectroscopy were applied.

#### 1. Chemicals and Materials

Commercial polycarbonate track-etched membranes with cylindrical pores (nominal pore diameter = 200 nm) were purchased from two different suppliers (Millipore Corporation, USA and Sterlitech Corporation, USA). The hydrophilic membranes exhibited the following technical specifications. Membranes obtained from Millipore belonged to the Isopore product range and according to the supplier possessed a surface-coating of polyvinylpyrrolidone (PVP) to improve their hydrophilicity. The porosity and water flow-rate in these filters were specified as 13.8% and 16 mL·min<sup>-1</sup>·cm<sup>-2</sup>, respectively. Filter membranes supplied by Sterlitech (pore  $\varnothing$  = 200 nm), in contrast, had a specified water flow-rate of 10 mL·min<sup>-1</sup>·cm<sup>-2</sup> and a pore density of 3·10<sup>8</sup> pores·cm<sup>-2</sup>, which corresponds to a porosity of 9.4 %. The manufacturer Sterlitech also employed PVP as a coating agent for the fabrication of hydrophilic track-etch membranes.

Both CaCl<sub>2</sub>·2H<sub>2</sub>O and (NH<sub>4</sub>)<sub>2</sub>CO<sub>3</sub> were obtained from Sigma-Aldrich and polyvinylpyrrolidone (PVP, M<sub>w</sub> = 1,300,000) was ordered from Alfa Aesar. All reagents were purchased in analytical grade and

applied without further purification. Deionised water (Milli-Q Standard, resistivity = 18.2 MΩcm) was used in the preparation of the reactant solutions.

## **2. Crystallisation Experiments**

### **2.1 Precipitation of CaCO<sub>3</sub> in Track-Etched Membranes**

CaCO<sub>3</sub> nanorods were precipitated within the cylindrical pores of track-etched membranes using the ammonium carbonate decomposition technique. Initially, the membranes were plasma-treated for 30 s to 1 min in order to remove organic impurities and to increase their hydrophilicity. The membranes were then transferred to glass vials containing 10 mL of a CaCl<sub>2</sub> solution (of concentration 0.5 mM, 10 mM or 100 mM) where they were degassed under reduced pressure to remove air bubbles from the pores. Subsequently, the filter membranes were kept in the calcium solution for 24 h to ensure complete wetting before being transferred to a closed desiccator, where 10 g of solid ammonium carbonate were placed at the bottom. In order to achieve slow diffusion conditions with respect to the gaseous decomposition products carbon dioxide and ammonia, the vials containing the reactant solution and the ammonium carbonate were both covered with Parafilm, which was punched with 5 needle holes. Crystallisation was typically allowed to proceed for 2 days before the intra-membrane material was extracted from the template.

After isolation from the reactant solution, the membranes were rinsed with cold water and ethanol. Subsequently, crystals precipitated on the surfaces of the membranes were removed by scraping with a glass cover slide. In order to achieve complete dissolution of the membranes, they were transferred to centrifuge tubes filled with 1.5 mL dichloromethane, briefly sonicated and subsequently centrifuged for 5 min at 14,500 rpm. Finally, the supernatant solution was removed and the dissolution-centrifugation cycle was repeated twice more followed by washing steps in methanol and ethanol. In preparation for further analysis, the precipitates were re-dispersed in ethanol and pipetted onto either glass cover slides for examination by SEM and vibrational spectroscopy or TEM grids (Cu grids coated with Formvar and evaporated carbon) for investigation using TEM. The CaCO<sub>3</sub> particles precipitated on the surfaces of the membranes were also examined using optical microscopy, SEM and Raman microscopy.

### **2.2 Effect of PVP on CaCO<sub>3</sub> Crystallisation**

A range of experiments were performed to confirm that no PVP was released from the membranes during crystallisation, thereby affecting the CaCO<sub>3</sub> polymorph.

**(1)** CaCO<sub>3</sub> was precipitated within the Sterlitech membranes in the presence of 0.5 g·L<sup>-1</sup> and 1 g·L<sup>-1</sup> PVP as a soluble organic additive ([Ca<sup>2+</sup>] = 10 mM).

(2) Membranes were immersed in deionised water for 3 days in order to remove water-soluble components from the surface before being used in the crystallisation experiments ( $[\text{Ca}^{2+}] = 10 \text{ mM}$ , additive-free conditions).

(3)  $\text{CaCO}_3$  was precipitated in bulk solution,  $[\text{Ca}^{2+}] = 10 \text{ mM}$ , in the presence of  $[\text{PVP}] = 1 \text{ g}\cdot\text{L}^{-1}$  using the ammonium carbonate decomposition method for 2 days. The crystals were grown on glass slides, which had previously been cleaned with Piranha solution (75 vol%  $\text{H}_2\text{SO}_4$  and 25 vol%  $\text{H}_2\text{O}_2$ ) and washed with Milli-Q water. After removal from the crystallisation solution, the glass substrates were rinsed in DI water as well as ethanol and left to dry. The crystals were then analysed using a range of methods to determine their sizes, morphologies and polymorphs.

### **2.3 Investigation of Early Stages in the Mineral Deposition**

In order to examine whether an amorphous precursor is involved in the infiltration of the track-etch membrane pores with calcium carbonate, samples were prepared as described in Section 2.1, but were removed from the desiccator after shorter periods of time (10 mins, 20 mins, 40 mins, 60 mins, 90 mins and 120 mins). For each time, the contents of 10 glass vials each containing 10 mL of reactant solution were combined, filtered through a polycarbonate membrane with 10 nm pores and the solid filter residues were quickly rinsed with ethanol to prevent the crystallisation of amorphous material. The precipitates were then analysed by Raman microscopy. For TEM studies, a small amount of the reactant solution was pipetted onto a TEM grid and rinsed with ethanol. Track-etch membranes, which had been placed in these reactant solutions during the exposure to ammonium carbonate vapour, were also observed by SEM to examine at what time their pores filled with mineral. Dissolving the templates (as described in Section 2.1) only yielded a visible amount of intra-membrane material after a reaction time of 2 hours.

In order to visualise the process of calcium carbonate precipitation, the reaction was also performed in a reduced volume under faster kinetics. For that purpose, a droplet of 10 mM calcium solution (200  $\mu\text{L}$ ) was pipetted onto a microscopy slide placed in a sealed petridish, which also contained a small amount of ammonium carbonate. The reaction was then followed by optical microscopy and the mineral deposits were examined under crossed polarizers to investigate their crystallinity.

### **3. Analysis of the Precipitates**

**Optical Microscopy.** The morphology and crystallinity of the  $\text{CaCO}_3$  crystals precipitated in bulk solution on glass slides or TE membranes were visually examined by the use of a Nikon Eclipse LV 100 polarisation microscope operated in the reflected light mode.

**Scanning Electron Microscopy (SEM) and Transmission Electron Microscopy (TEM).** SEM images were recorded with a LEO 1530 Gemini FEG-SEM instrument operated at an acceleration voltage of 3 kV in high vacuum. The images were collected in the in-lens detector mode. Prior to their examination in the electron microscope, the glass substrates supporting the precipitates were attached to Al stubs holders with adhesive carbon pads. All samples were coated with 5 nm or 10 nm Pd/Pt alloy by the use of an Agar high resolution sputter coater. TEM and selected area electron diffraction (SAED) were performed on an FEI Technai TF20 FEGTEM operating at 200 kV. The instrument was equipped with a Gatan Orius SC600A CCD camera.

**Vibrational Spectroscopy.** Raman microscopy was carried out using a Renishaw 2000 inVia instrument equipped with a 785 nm diode laser. A 50x objective (numerical aperture NA 0.75) was used to focus the laser onto the sample. Spectra were typically recorded in the wavenumber range of 100 – 1200  $\text{cm}^{-1}$  at 0.1% laser power. Infra-red spectroscopy of powders was performed with a Perkin Elmer AT-IR spectrometer.

#### **4. Characterisation of the Track-Etched Membranes**

The surface chemistries and topographies of the different membranes were studied using a range of analytical techniques.

**Vibrational Spectroscopy.** For Raman and infra-red spectroscopy, the membranes were folded 3 times to increase the volume of material inserted into the beam path. In the case of Raman experiments, the membranes were fixed on a microscopy slide using Sellotape. Spectra were then recorded on the same instruments as specified for the analysis of the precipitates.

**Scanning Electron Microscopy (SEM).** In preparation for SEM, the different membranes were mounted on aluminium sample holders using conducting tape. The specimens were then coated with a 10 nm thick film of Pt/Pd alloy and examined as described above.

**X-ray Photoelectron Spectroscopy (XPS).** XPS measurements were performed using a VG Escalab 250 XPS with monochromated aluminium K-alpha x-ray source. The spot size was 500  $\mu\text{m}$  with a power of 150W. Detailed spectra of individual peaks were taken at energy of 20 eV with a step size of 0.1 eV. Binding energy was calibrated by setting the carbon 1s peak to 285 eV. Detailed spectra had a Shirley or linear background fitted to them and peaks were fitted and deconvoluted using mixed Gaussian-Lorentzian fits (using CASAXPS). The standard error was estimated by triplicate measurements of the same sample.

**BET Analysis.** Surface area analysis based on the method by Brunauer, Emmett and Teller (BET) was carried out using a Micrometrics ASAP 2020, Nitrogen Sorption instrument using 250 mg – 500 mg of membrane material. Prior to the gas adsorption measurements, the samples were degassed at 40°C for 12 hours. A total of 13 data points were recorded and 3 repeats were run for each type of specimen in order to estimate standard errors. Fractal dimensions  $D_s$  were derived from the nitrogen adsorption curves according to the Frankel-Halsey-Hill (FHH) method.<sup>2,3</sup> These evaluations are based on the following equation, where  $V$  represents the adsorbed gas volume at a relative pressure of  $P/P_0$ .

$$\ln\left(\frac{V}{V_m}\right) = \text{const.} + \frac{1}{s} \ln\left(\ln\left(\frac{P_0}{P}\right)\right)$$

$$s > 3; \frac{1}{s} = \frac{(3 - D_s)}{3}$$

$$s < 3; \frac{1}{s} = 3 - D_s$$

Only data points in the region of statistical multilayer adsorption with  $0.01 < P/P_0 < 0.18$  were considered in the fractal analysis.

**Atomic Force Microscopy (AFM).** The surface topographies the membranes were analysed using a NanoMan instrument (Veeco). All images were collected at room temperature in the tapping mode (scan rate = 1.98 Hz) using antimony (n) doped silicon tips (purchased from Bruker Tespa), which exhibited typical resonance frequencies of 345 - 385 kHz and force constants of 20 - 80 N/m. Fractal dimensions were extracted from the images (resolution 512 x 512 pixels) applying the lake/island perimeter-area method as described by Williams *et al.* (box size to 375 nm).<sup>4</sup>

## (2) Supplementary Figures

**Figure S1:** SEM images of representative 200 nm Millipore track-etch membranes after mineralisation in the absence of organic additives ( $[Ca^{2+}] = 10$  mM). (a)  $CaCO_3$  rods were present in approximately 80% of the pores. (b) The roughly circular cross section of the mineral particles is dictated by the structural features of the template. Bulk crystals deposited on the surface of the filter membrane have been removed prior to imaging.

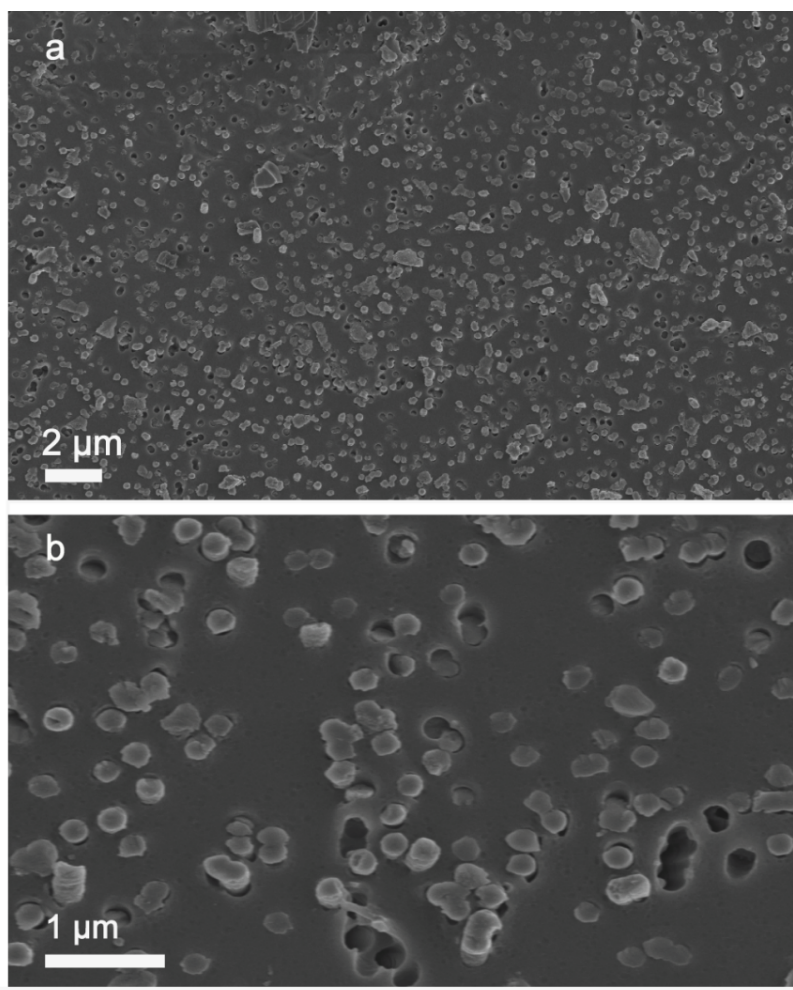


**Figure S2:** Raman spectrum of a powder of  $\text{CaCO}_3$  nano-rods precipitated in 200 nm Millipore membrane pores. The distinctive peaks at  $1090\text{ cm}^{-1}$  and  $1075\text{ cm}^{-1}$  ( $\nu_1$ , carbonate symmetric stretching) are characteristic of vaterite (V).<sup>5</sup> Only these most intense vibration bands in the  $\text{CaCO}_3$  spectrum are unequivocally identifiable due to the small amount of sample available and the additional presence of residual polycarbonate originating from the dissolved membrane material.

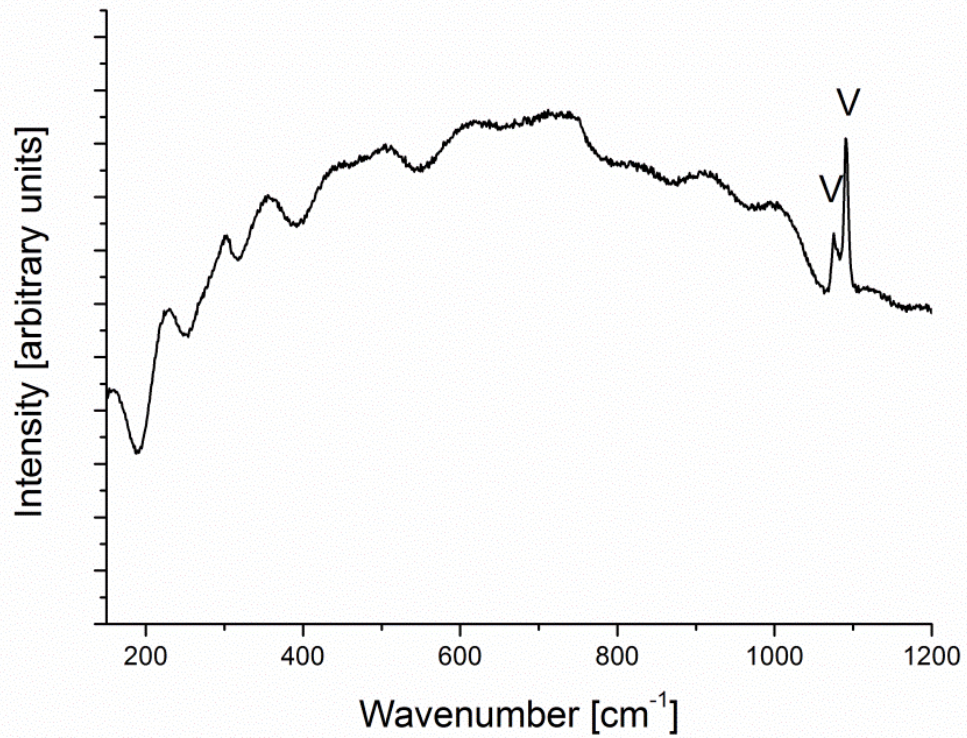


**Figure S3.** SEM images of  $\text{CaCO}_3$  crystals precipitated on the surfaces of TE membranes with pore diameters of 200 nm. Rhombohedral calcite crystals (c) are principally formed, together with a minor fraction of vaterite (V). (a) The Millipore membranes, which promote vaterite precipitation within their pores, do not show an increased proportion of vaterite on their surfaces as compared with the Sterlitech membranes (b).

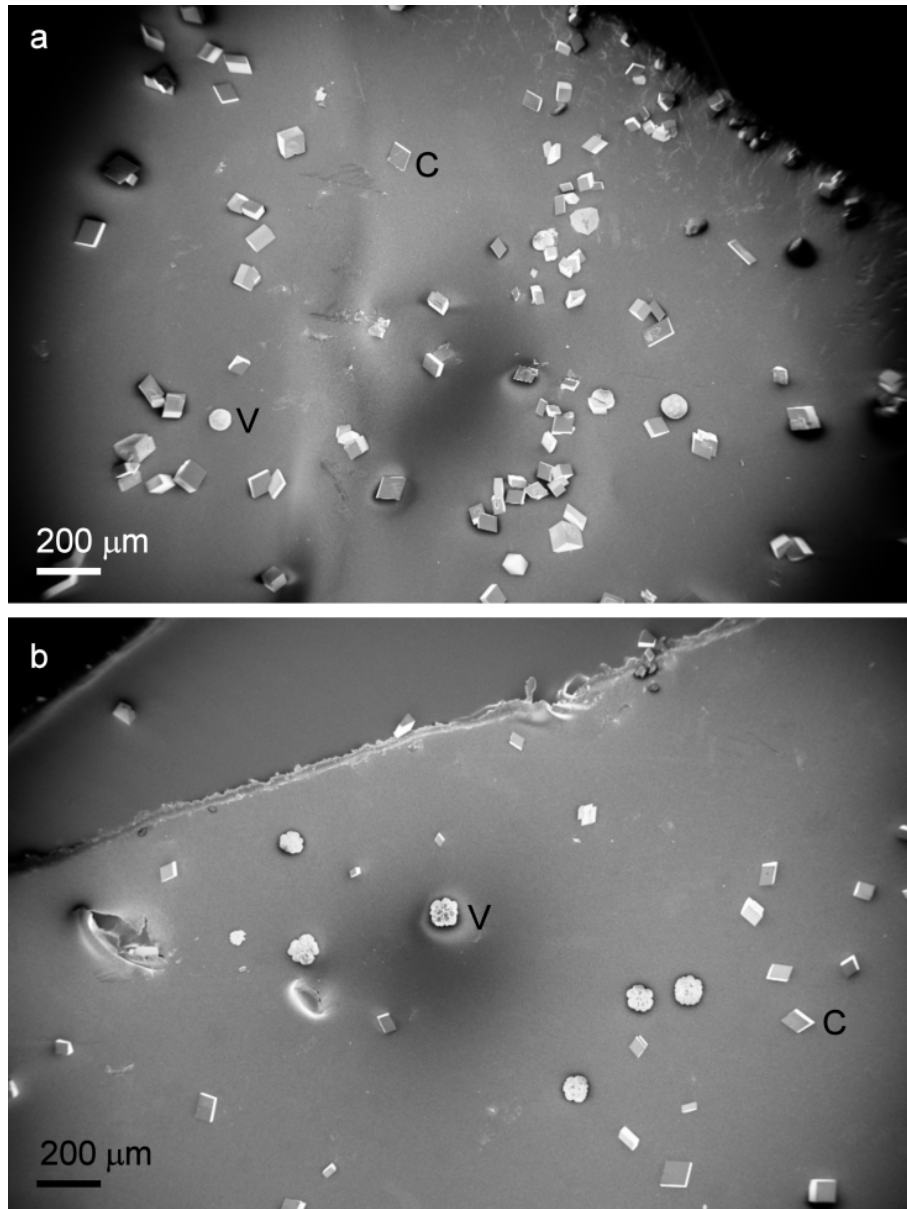


**Figure S4.** TEM and selected area electron diffraction patterns of nano-rods precipitated in 200 nm Sterlitech TE membranes at  $[Ca^{2+}] = 100$  mM. (a) A representative rod-shaped particle grown within a track-etch membrane pore. The length of the rod corresponds to the thickness of the template, indicating good infiltration under the high supersaturation conditions. (b) The intra-membrane particles appear solid, and (c,d) electron diffraction patterns taken from different areas along the same rod confirm that they are uniformly vaterite. The crystallinity, however, varies along the rod. While in some areas there are only minor deviations from single-crystallinity (c) other regions are clearly polycrystalline (d).

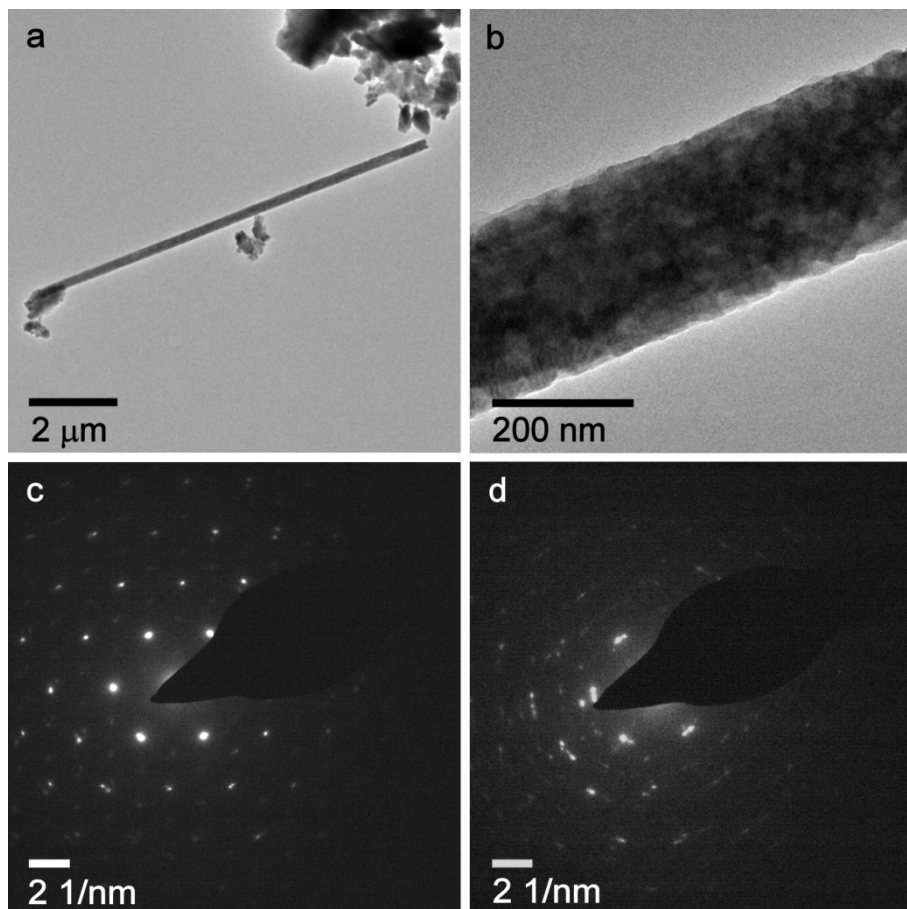


**Figure S5.** TEM images of  $\text{CaCO}_3$  nanorods precipitated in 200 nm Millipore membranes at  $[\text{Ca}^{2+}] = 100 \text{ mM}$ . (a) Rod-like crystals of vaterite were obtained in high yield, as confirmed by electron diffraction (b). Most rods were single crystals, although some polycrystalline domains were sometimes observed. (c) The vaterite rods appear solid, and their lengths indicate that they entirely fill the pores. (d) A granular substructure is clearly visible at the ends of some of the rods.

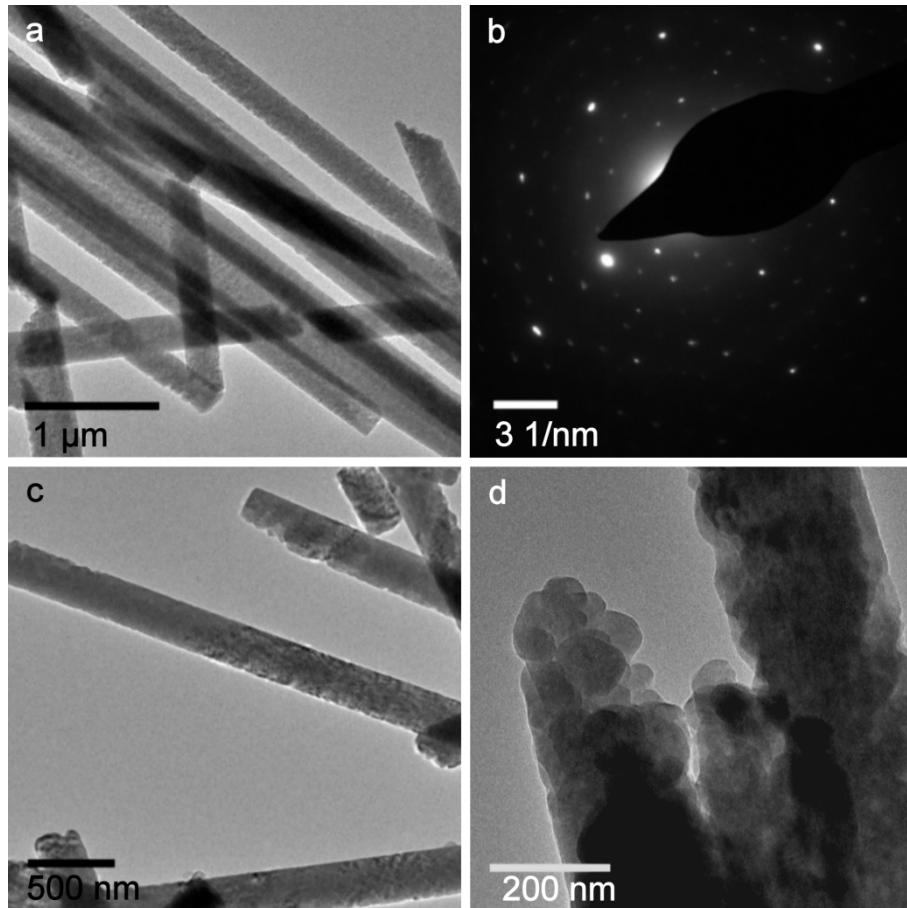


**Figure S6.** Calcium carbonate precipitated in the presence of  $1 \text{ g}\cdot\text{L}^{-1}$  poly(vinylpyrrolidone) (PVP) and  $10 \text{ mM CaCl}_2$  using the ammonium carbonate method. (a) Light microscopy images of rhombohedral calcite produced after 2 days and (b) SEM images of these crystals. The inset in (a) shows the chemical structure of polyvinylpyrrolidone.

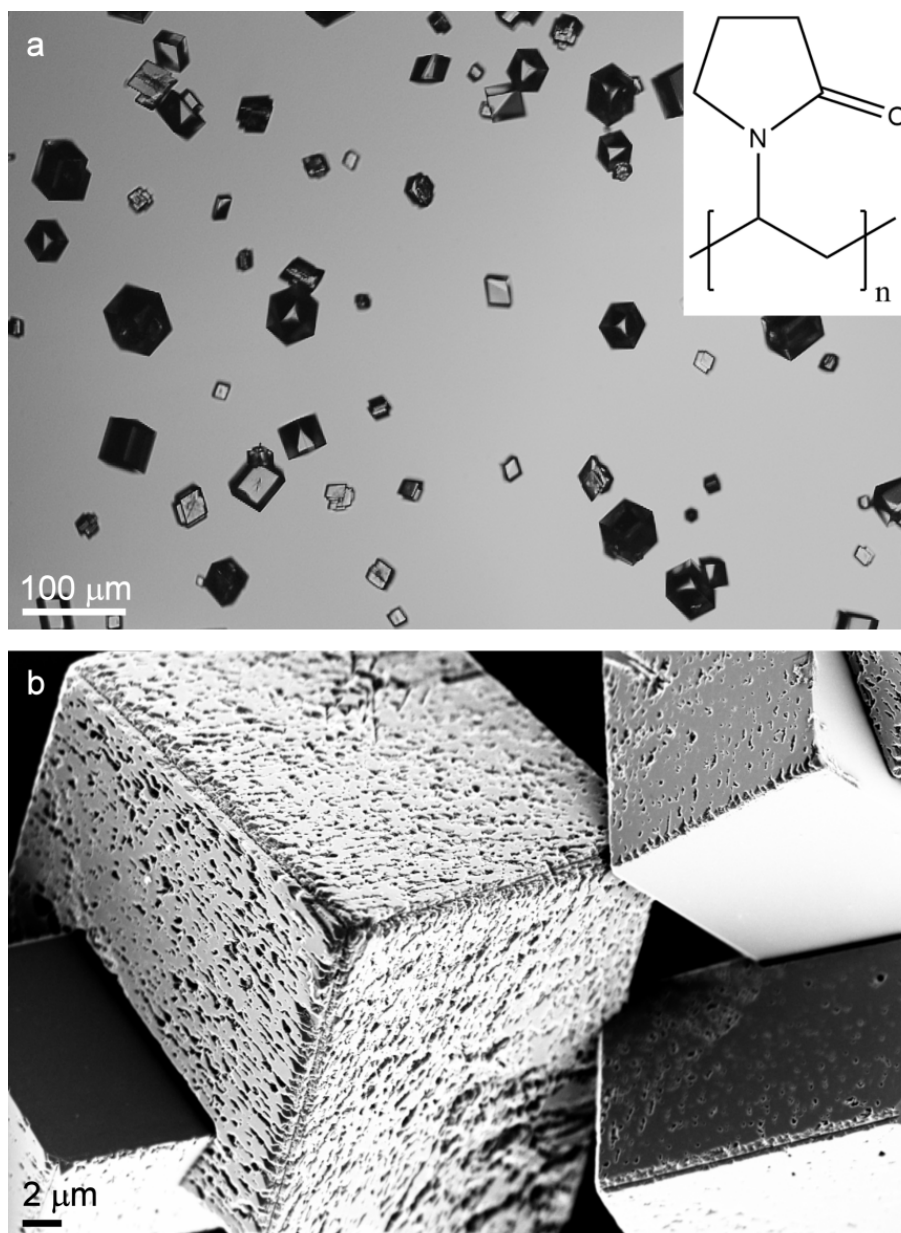


**Figure S7.** SEM images of track etch membranes with 200 nm pores, purchased (a) from Millipore and (b) from Sterlitech. Both show similar pore size distributions. In some cases adjacent pores are fused together, and the Millipore membranes exhibit a slightly higher pore density.

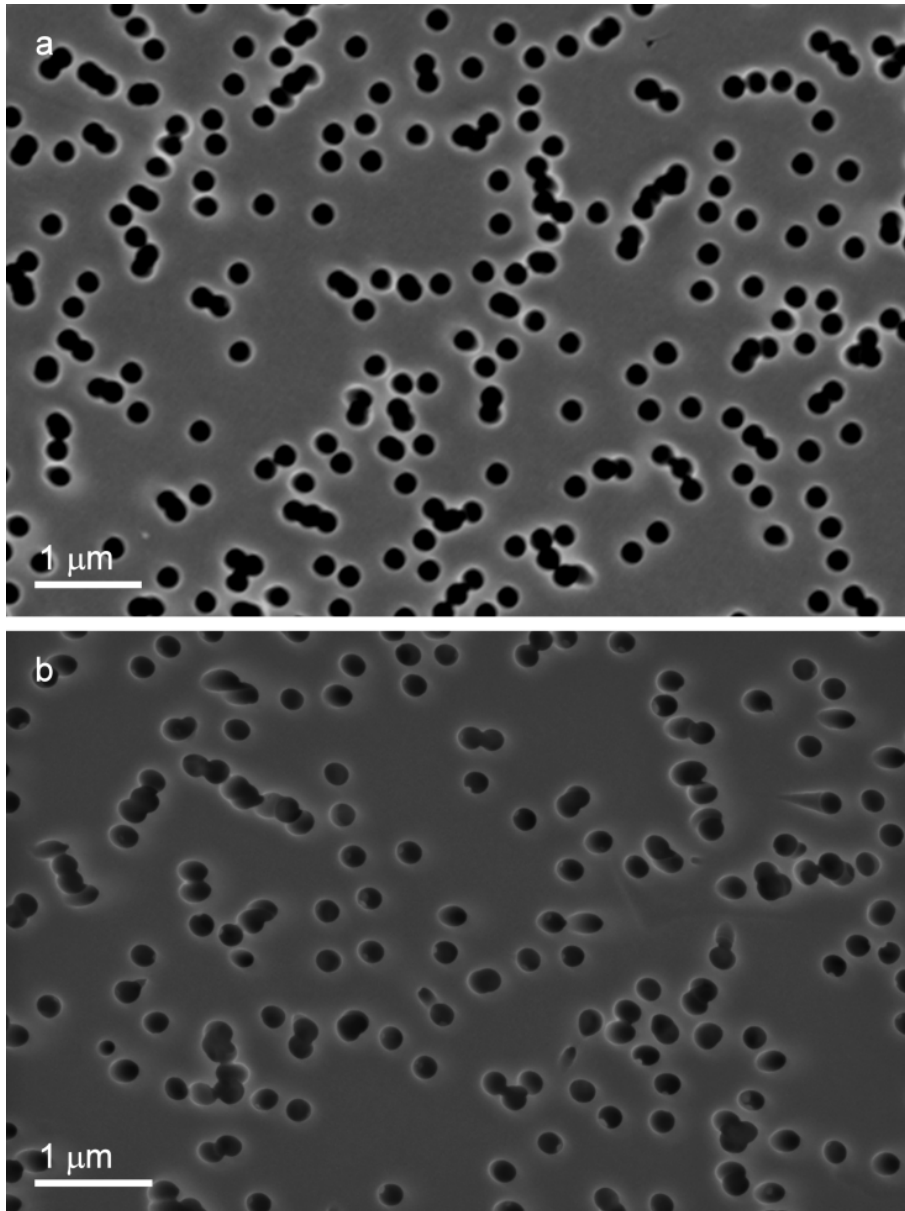


**Figure S8.** (a) IR and (b) Raman spectra of (i) Sterlitech membranes (200 nm pores), (ii) Millipore membranes (200 nm pores). All of the bands in the spectra can be assigned to polycarbonate.

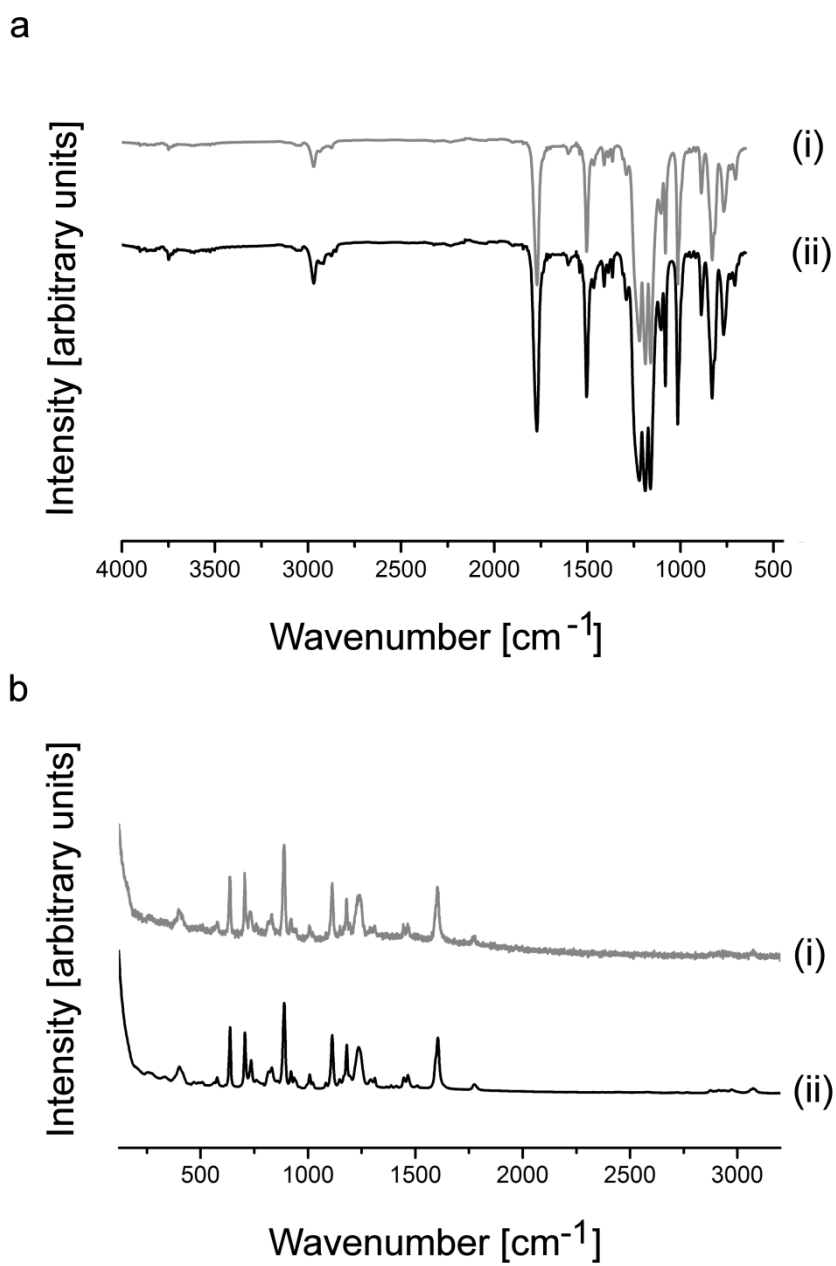


**Figure S9.** BET nitrogen adsorption isotherms for 200 nm Millipore and Sterlitech membranes. The curves each represent an average over 3 individual measurements. Only the region of multilayer adsorption (data points with  $0.01 < P/P_0 < 0.18$ ) were considered for the calculation of fractal dimensions.

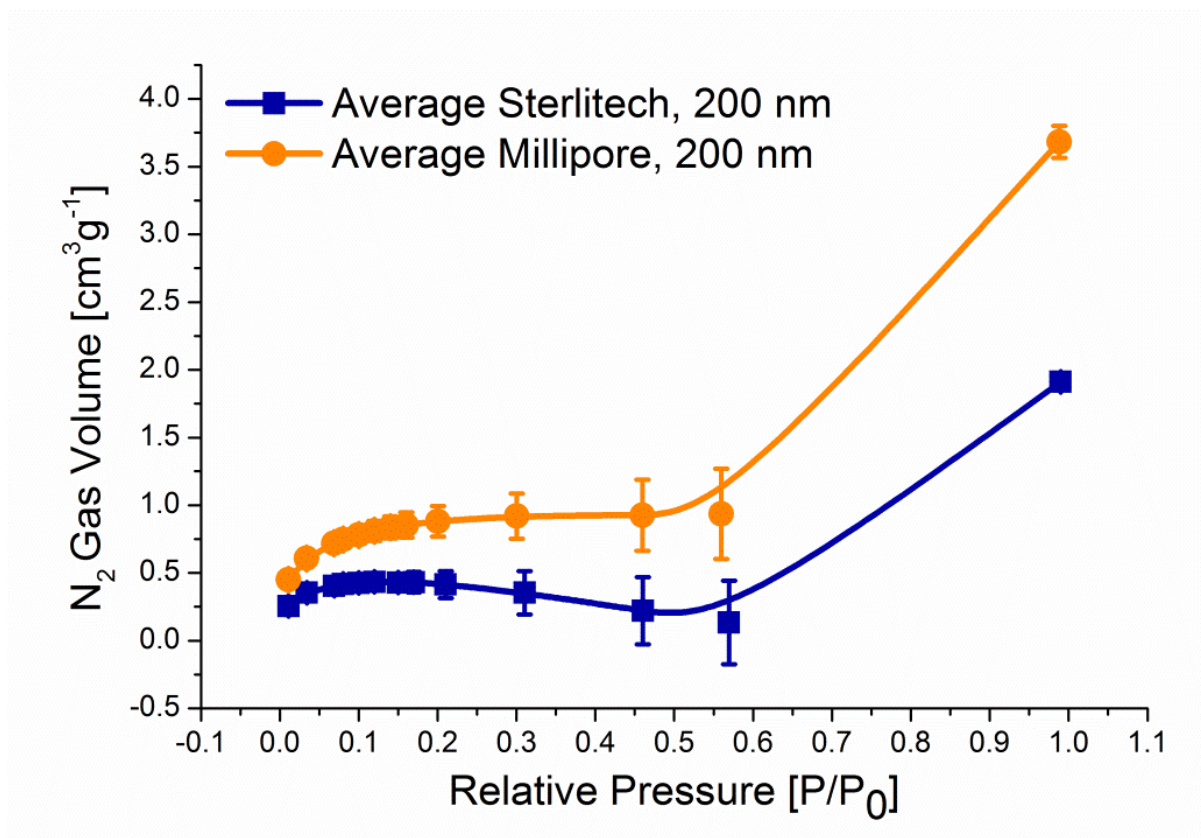


**Figure S10.** Atomic force microscopy (AFM) images of the surfaces of track-etched membranes with 200 nm pores. The Millipore membranes (a) exhibit a higher root mean-square roughness ( $R_q = 2.18$  nm) than those from Sterlitech (b), for which a value of  $R_q = 0.95$  nm was calculated.

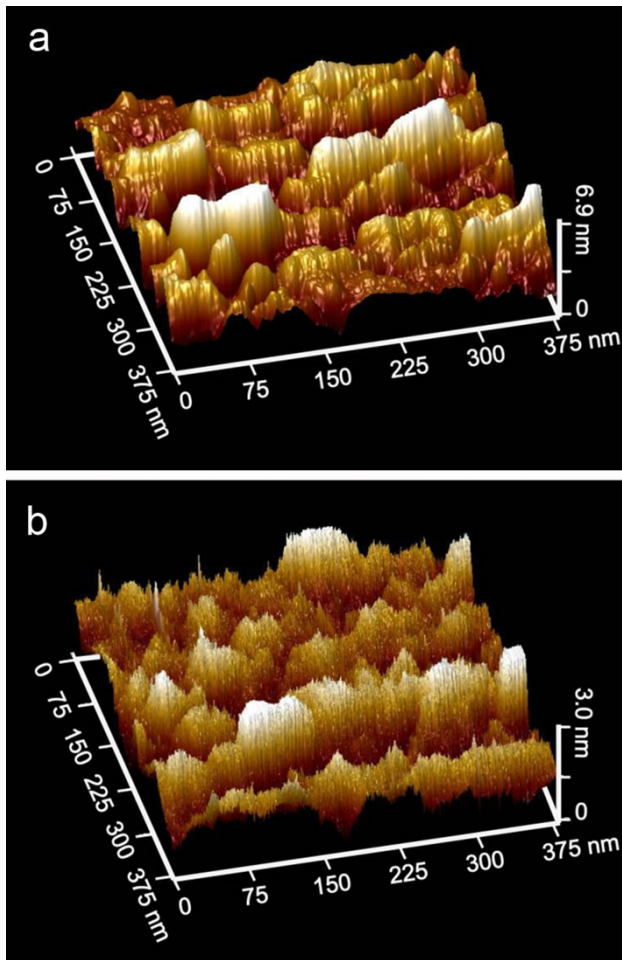
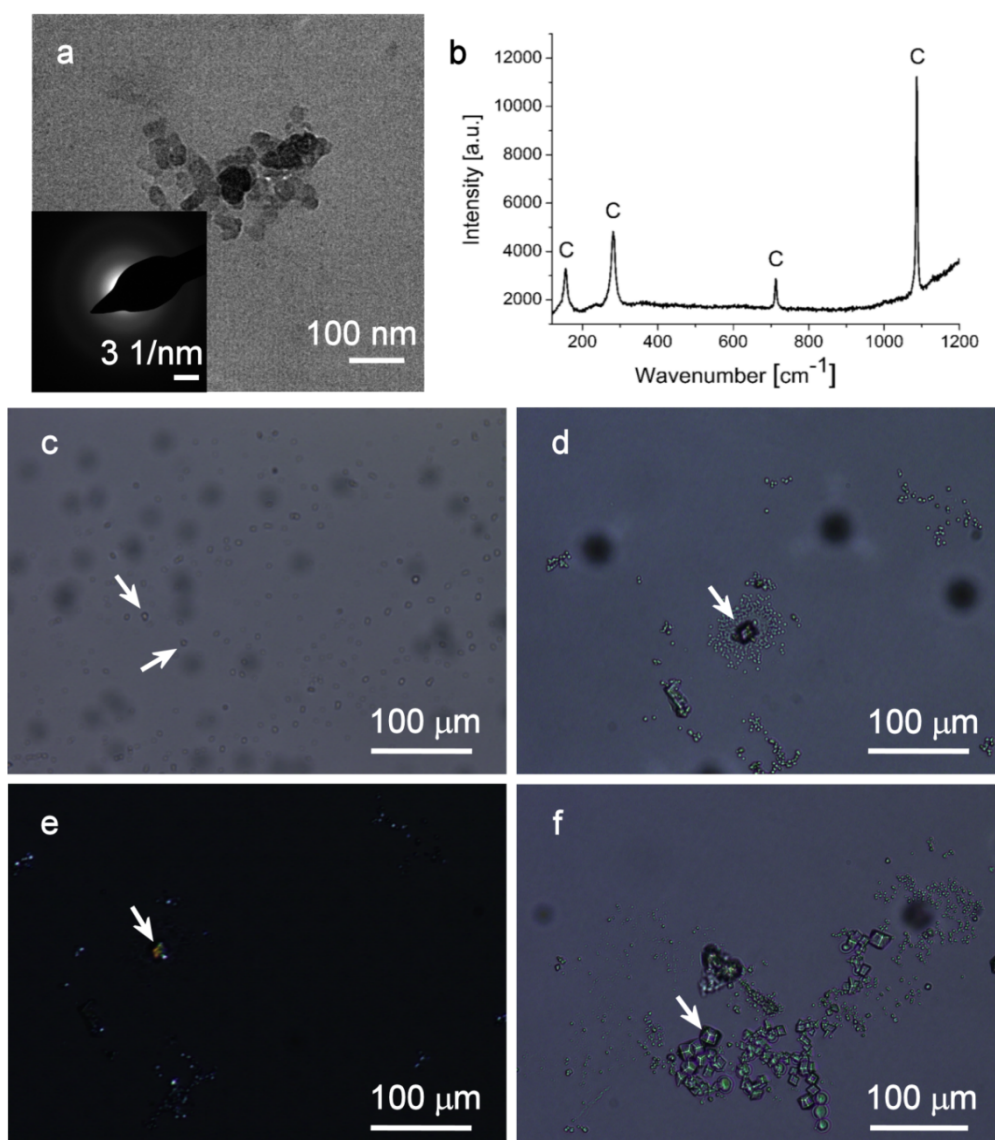


**Figure S11.** Early stages in the precipitation of  $\text{CaCO}_3$  from a 10 mM  $\text{CaCl}_2$  solution. (a, b) Samples were drawn from the reactant solution at different stages of the reaction. TEM shows that after 60 mins of exposure to ammonium carbonate vapour a minor amount of amorphous calcium carbonate can still be identified in the precipitate (a), while most of the deposited material is already crystalline calcite. (b) After a reaction time of 90 mins, when there is still no infiltration of the TE membrane pores visible in SEM, Raman microscopy confirms that all bulk material recovered from the solution is calcite. (c-f) The mineral deposition was also visually followed by optical microscopy in a small reaction volume of 200  $\mu\text{L}$  on a glass slide placed in a closed petridish with ammonium carbonate. Images representative of the sample were collected after (c) 5 mins, (d, e) 8 mins and (f) 12 mins. In the very early stages ( $\leq 5$ mins) spherical, non-crystalline aggregates are observed (c) indicating that amorphous calcium carbonate is deposited initially. After 8 mins crystalline material is seen (d) as confirmed by its bright appearance under crossed polarizers (e). (f) Eventually, most of the precipitate is transformed into rhombohedral calcite crystals.



### (3) Supplementary Tables

**Table S1:** Relative elemental abundance determined by x-ray photoelectron spectroscopy (XPS).

Sample	C 1s %	Cl 2p %	N 1s %	Na 1s %	O 1s %	S 2p %
Millipore 200 nm	84.5	0.0	3.3	0.1	11.8	0.3
Sterlitech 200 nm	85.0	0.1	3.0	0.2	11.4	0.2

**Table S2:** Speciation of the chemical environment of the carbon atoms present within the membrane materials based on the binding energy of the 1s orbital.

Sample	Carbon atom	Position	% Concentration	Speciation
Millipore 200 nm	C 1s - a	285.0038	65	aliphatic and aryl
	C 1s - b	286.2637	28	higher energy oxygenated species
	C 1s - c	287.6102		
	C 1s - d	290.9917	7	carbonate species
	C 1s - e	292.4217		
Sterlitech 200 nm	C 1s - a	284.9919	63	aliphatic and aryl
	C 1s - b	286.2602	31	higher energy oxygenated species
	C 1s - c	287.6587		
	C 1s - d	291.0073	6	carbonate species
	C 1s - e	292.4229		

#### **(4) Characterisation of Track-Etch Membranes**

In this section further details about the characterization of the different polycarbonate membranes are provided.

##### **Chemical Composition of the Membrane Surfaces Studied by Vibrational Spectroscopy and X-ray Photoelectron Spectroscopy (XPS).**

IR and Raman showed bands consistent with polycarbonate only<sup>6, 7</sup> and no surface coating or differences in the bulk material were identified (Figure S8). X-ray photoelectron spectroscopy (XPS) was performed to analyse the chemical composition of the membrane surfaces, where this surface-sensitive technique provides information about the binding energy of electrons from the uppermost 10 nm thick layer of the sample. The relative abundances of the elements detected in the membranes are summarised in Table S1, where a slightly higher proportion of nitrogen species in the Millipore membrane was identified. However, given a standard error of 0.5 at%, this difference cannot be considered statistically significant. Detailed evaluation of the chemical environment of the carbon species in the XPS spectra also enables characterisation of functional groups present on the membranes (Table S2). The vast majority of the carbon atoms on the surfaces of the membranes were bound in aryl rings and aliphatic chains as it is expected for polycarbonate, suggesting no major differences in the surface chemistries of the membrane. However, due to the geometry of the experiments, it should be noted that the XPS data were principally obtained from the outer surfaces of the membranes and we cannot rule out that differences could not occur within the membrane pores.

##### **Surface Roughness Studied by BET and Atomic Force Microscopy (AFM).**

Gas adsorption (BET) and atomic force microscopy (AFM) measurements were used to characterise the topographies of the membranes. BET revealed that the Millipore membranes had slightly higher surface areas ( $2.8 \pm 0.02 \text{ m}^2 \text{ g}^{-1}$  (Millipore) vs.  $1.8 \pm 0.50 \text{ m}^2 \text{ g}^{-1}$  (Sterlitech)), as is consistent with the higher pore density in the former. Providing a quantitative measure for the irregularity and roughness of pore surfaces<sup>8</sup>, the surface fractal dimension  $D_s$  was extracted from each BET data set. This parameter can adopt values between 2 and 3. While a fractal dimension of 2 is characteristic of a perfectly smooth surface, a value of 3 corresponds to a sponge-like structure. Fractal analysis of the nitrogen adsorption isotherms depicted in Figure S9 according to the Frankel-Halsey-Hill

theory<sup>2,3</sup> yielded fractal indices of  $D_s = 2.23 \pm 0.024$  for membranes purchased from Sterlitech and  $D_s = 2.43 \pm 0.066$  for those from Millipore. The differences in the fractalities of the surfaces are therefore very minor.

This observation was further confirmed by AFM analysis (Figure S10). AFM showed that the surfaces of the Millipore membranes were slightly rougher than those from Sterlitech, as quantified by a root mean-square roughness of  $R_q = 2.18$  nm as compared to  $R_q = 0.95$  nm. Fractal indices were also calculated from the AFM images using the lake/island perimeter-area method,<sup>4</sup> giving values of  $D_s = 2.11$  (Sterlitech) and  $D_s = 2.36$  (Millipore). The parameters derived using AFM are therefore in good agreement with those extracted from the BET isotherms, where it is noted that the AFM measurements sample the outer surface of the membranes, whereas the BET curves are dominated by the structural features of the membrane pores.

### (5) Early Stage Analysis of Precipitation Mechanism

At the concentrations employed here, ACC is the first phase to precipitate from the reaction solution, as demonstrated by optical microscopy and TEM/SAED (Fig. S11). However, the amorphous precursor was only detectable in small amounts during the first 60 minutes of the reaction, such that it was not possible to isolate significant amounts for further analysis even at early stages of the reaction. Polarised optical microscopy was therefore used to demonstrate the presence of ACC *in situ* within the reaction solution at early stages and was observed to be consumed during the formation of calcite rhombohedra (Fig. S11). SEM imaging of polycarbonate membranes removed from the reaction after different periods of time first showed a visible filling of the template pores ( $\approx$  80% pores infiltrated) with mineral after 2 hours, when all bulk material had already crystallised to calcite as evidenced by Raman microscopy (Fig. S11).

### References

1. Y.-Y. Kim, N. B. J. Hetherington, E. H. Noel, R. Kröger, J. M. Charnock, H. K. Christenson and F. C. Meldrum, *Angew. Chem. Int. Ed.*, 2011, **50**, 12572-12577.
2. D. Avnir and M. Jaroniec, *Langmuir*, 1989, **5**, 1431-1433.
3. H. Fei, H. Xiaodong and L. Yao, in *1st IEEE International Conference on Nano/Micro Engineered and Molecular Systems. NEMS '06*, 2006, pp. 1272-1275.
4. J. M. Williams and T. P. Beebe, *J. Phys. Chem.*, 1993, **97**, 6255-6260.
5. U. Wehrmeister, A. L. Soldati, D. E. Jacob, T. Häger and W. Hofmeister, *J. Raman Spectrosc.*, 2010, **41**, 193-201.
6. R. G. Kraus, E. D. Emmons, J. S. Thompson and A. M. Covington, *J. Polym. Sci. Part B Polym. Phys.*, 2008, **46**, 734-742.

7. S. N. Lee, V. Stolarski, A. Letton and J. Laane, *J. Mol. Struct.*, 2000, **521**, 19-23.
8. Q. Wei and D. W. Wang, *Mater. Lett.*, 2003, **57**, 2015-2020.